ITP-Budapest 590, DESY 02-145

Z-Burst Scenario for the Highest Energy Cosmic Rays*

Z. Fodor
Institute for Theoretical Physics, Eötvös University, Budapest, Pázmány 1/a, H-1117

S.D. Katz[†]**, A. Ringwald**
Deutsches Elektronen-Synchrotron DESY, Hamburg, Notkestraße 85, D-22607

Abstract. The origin of highest energy cosmic rays is yet unknown. An appealing possibility is the so-called Z-burst scenario, in which a large fraction of these cosmic rays are decay products of Z bosons produced in the scattering of ultrahigh energy neutrinos on cosmological relic neutrinos. The comparison between the observed and predicted spectra constrains the mass of the heaviest neutrino. The required neutrino mass is fairly robust against variations of the presently unknown quantities, such as the amount of relic neutrino clustering, the universal photon radio background and the extragalactic magnetic field. Considering different possibilities for the ordinary cosmic rays the required neutrino masses are determined. In the most plausible case that the ordinary cosmic rays are of extragalactic origin and the universal radio background is strong enough to suppress high energy photons, the required neutrino mass is $0.08\,\text{eV} \leq m_\nu \leq 0.40\,\text{eV}$. The required ultrahigh energy neutrino flux should be detected in the near future by experiments such as AMANDA, RICE or the Pierre Auger Observatory.

1. Introduction

The existence of a background gas of free photons and neutrinos is predicted by cosmology. The measured cosmic microwave background (CMB) radiation supports the applicability of standard cosmology back to photon decoupling which occured approximately one hundred thousand years after the big bang. The relic neutrinos have decoupled much earlier, when the universe had a temperature of one MeV and the age of just one second. Thus, a measurement of the relic neutrinos would provide a new window to the early universe. The predicted average number density of relic neutrinos per light ($m_{\nu_i} \ll 1$ MeV) species i is $\simeq 56$ cm^{-3}. This density is comparable with that of photons. However, since neutrinos interact only weakly, the relic neutrinos have not yet been detected.

Recently, an indirect detection possibility for relic neutrinos has been discussed [1–5]. It is based on so-called Z-bursts resulting from the resonant annihilation of ultrahigh energy cosmic neutrinos (UHECνs) with relic neutrinos into Z bosons (cf. Fig. 1). The decay products of the Z may be detected and yield thereby indirect evidence for the existence of relic neutrinos.

According to recent oscillation measurments (see e.g. [6–9]), neutrinos have non-vanishing masses, m_{ν_i}. In this case the resonant energy at which the Z production cross-section is sizeable reads

$$E_{\nu_i}^{\text{res}} = \frac{M_Z^2}{2\,m_{\nu_i}} = 4.2 \cdot 10^{21}\ \text{eV} \left(\frac{1\ \text{eV}}{m_{\nu_i}}\right) , \tag{1}$$

*Talk given at Beyond the Desert '02, Oulu, Finland, June 2-8, 2002.
[†]On leave from Institute for Theoretical Physics, Eötvös University, Pázmány 1, H-1117 Budapest, Hungary

where M_Z is the mass of the Z boson. For neutrino masses of $\mathcal{O}(1)$ eV the resonant energy is remarkably close to the energies of the highest energy cosmic rays observed at Earth by collaborations such as AGASA [10], Fly's Eye [11–13], Haverah Park [14, 15], HiRes [16], and Yakutsk [17] (for a review, see Ref. [18]). The possibility that the ultrahigh energy cosmic rays (UHECRs) may originate from Z-bursts was first discussed in [4, 5].

One of the most outstanding puzzles in cosmic ray physics is the existence of cosmic ray events above the Greisen-Zatsepin-Kuzmin (GZK) cutoff [19, 20]. The energy spectrum of ultrahigh energy cosmic rays is expected to show a cutoff around $4 \cdot 10^{19}$ eV which is not conclusively seen in the data [21]. With the help of the Z-burst scenario one can not only detect the relic neutrino background indirectly but also explain the existence of the highest energy cosmic rays [22–40].

The comparison between the observed and predicted UHECR spectra gives constraints on the mass of the heaviest neutrino [32–34, 36]. In this review our quantitative analysis of the Z-burst scenario is presented. The requried mass of the heaviest neutrino, as well as the necessary UHEν flux is determined.

The organization of this review is as follows. The next section summarizes our present knowledge on neutrino masses. Section 3 gives the produced spectrum of protons and photons from Z-bursts. The comparison with the observed spectrum is presented in Section 4 and the conclusion is given in Section 5.

2. Neutrino masses

According to recent experiments, neutrinos almost certainly have non-vanishing masses and mixing angles. The evidence for neutrino oscillation is compelling for atmospheric neutrinos [6], strong for solar neutrinos [7, 8], and so-far unconfirmed for neutrinos produced in the laboratory and studied by e.g. the LSND collaboration [9]. However, neutrino oscillations are sensitive only to the mass (squared) differences $\triangle m^2_{ij} = m^2_{\nu_i} - m^2_{\nu_j}$, not to the individual masses, $(m_{\nu_4} >) \, m_{\nu_3} > m_{\nu_2} > m_{\nu_1}$, themselves. Only a lower bound on the mass of the heaviest neutrino can be derived from these observations, e.g.

$$m_{\nu_3} \geq \sqrt{\triangle m^2_{\rm atm}} \gtrsim 0.04 \, {\rm eV} \tag{2}$$

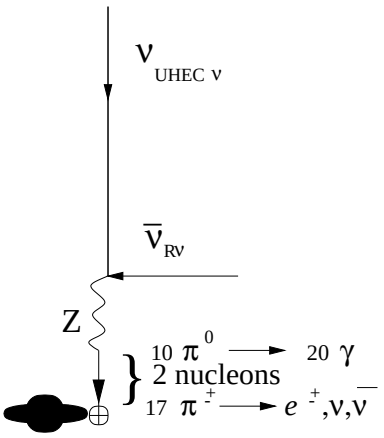

Figure 1. Illustration of a Z-burst resulting from the resonant annihilation of an ultrahigh energy cosmic neutrino on a relic (anti-)neutrino. (Adapted from Ref. [30].)

from the atmospheric mass splitting in a three neutrino flavour scenario and

$$m_{\nu_4} \geq \sqrt{\triangle m^2_{\rm LSND}} \gtrsim 0.4 \, {\rm eV} \tag{3}$$

from the still allowed value of the LSND mass splitting in a four flavour scenario.

For an investigation of the absolute scale of neutrino masses one has to exploit different types of experiments, such as the search for mass imprints in the endpoint spectrum of tritium beta (β) decay or the search for neutrinoless double beta ($0\nu2\beta$) decay. At present, these direct kinematical measurements of neutrino masses provide only upper limits, e.g.

$$m_\beta \equiv \sqrt{\sum_i |U_{ei}|^2 \, m^2_{\nu_i}} < 2.2 \div 2.5 \, {\rm eV} \quad (95\,\%\ {\rm C.L.}) \, , \tag{4}$$

with U being the leptonic mixing matrix, for the effective mass measured in tritium β decay [41–43], and

$$\langle m_\nu \rangle \equiv \left| \sum_i U^2_{ei} \, m_{\nu_i} \right| < 0.33 \div 1.35 \, {\rm eV} \quad (90\,\%\ {\rm C.L.}) \tag{5}$$

for the Majorana neutrino mass parameter [44, 45] appearing in $0\nu2\beta$ decay. Recently an evidence for neutrinoless double beta decay was reported [46]. The corresponding neutrino mass range is:

$$\langle m_\nu \rangle = (0.11 \div 0.56) \, {\rm eV} \quad (95\,\%\ {\rm C.L.}) \tag{6}$$

Combining the experimental constraints from oscillations and from tritium β decay, one infers upper bounds on the mass of the heaviest neutrino,

$$m_{\nu_3} < \sqrt{m^2_\beta + \triangle m^2_{\rm atm}} \lesssim 2.5 \, {\rm eV} \, , \tag{7}$$

in a three flavour, and

$$m_{\nu_4} < \sqrt{m^2_\beta + \triangle m^2_{\rm LSND}} \lesssim 3.8 \, {\rm eV} \, , \tag{8}$$

in a four flavour scenario.

Further information on the absolute scale of neutrino masses can be obtained through cosmological and astrophysical considerations. Neutrinos in the $0.1 \div 1$ eV mass range have cosmological implications since they represent a non-negligible part of dark matter. This gives the opportunity to put upper limits on neutrino masses from cosmology [47–50]. A recent galaxy redshift survey gives an upper bound

$$\sum_i m_{\nu_i} < 1.8 \, {\rm eV} \tag{9}$$

on the sum of the neutrino masses [51]. From the spread of arrival times of neutrinos from supernova SN 1987A, coupled with the measured neutrino energies, a time-of-flight limit of $m_\beta < 23$ eV can be derived [53, 54], which, however, is not competitive with the direct limit (4). According to a recent study, leptogenesis requires that all the neutrinos have masses smaller than 0.2 eV [55].

3. Z-burst spectra

The calculation of the Z-burst spectra of protons and photons was performed in three steps. First, we determined the probability of Z production as a function of the distance from Earth. Secondly, using results from collider experiments we derived the energy distribution of the produced protons and photons in the laboratory (lab) system. As a last step the energy losses due to the propagation of the protons and photons were taken into account.

The prediction of the differential proton flux, i.e. the number of protons arriving at Earth with energy E per units of energy (E), of area (A), of time (t) and of solid angle (Ω),

$$F_{p|Z}(E) = \frac{\mathrm{d}N_{p|Z}}{\mathrm{d}E\,\mathrm{d}A\,\mathrm{d}t\,\mathrm{d}\Omega}\,, \tag{10}$$

from Z-bursts can be summarized as

$$\begin{aligned} F_{p|Z}(E) = \sum_i \int_0^\infty \mathrm{d}E_p \int_0^{R_{\max}} \mathrm{d}r \\ \times \left[\int_0^\infty \mathrm{d}E_{\nu_i}\, F_{\nu_i}(E_{\nu_i}, r)\, n_{\bar{\nu}_i}(r) + \int_0^\infty \mathrm{d}E_{\bar{\nu}_i}\, F_{\bar{\nu}_i}(E_{\bar{\nu}_i}, r)\, n_{\nu_i}(r) \right] \\ \times \sigma_{\nu_i\bar{\nu}_i}(s)\,\mathrm{Br}(Z \to \mathrm{hadrons})\,\frac{\mathrm{d}N_{p+n}}{\mathrm{d}E_p}(-)\frac{\partial}{\partial E}P_p(r, E_p; E)\,, \end{aligned} \tag{11}$$

with the following important building blocks: the UHECν fluxes $F_{\nu_i}(E_{\nu_i}, r)$ at the energies E_{ν_i} ($\approx E_{\nu_i}^{\mathrm{res}}$) and at the distance r of Z production to Earth, the number density $n_{\nu_i}(r)$ of the relic neutrinos, the Z production cross section $\sigma_{\nu_i\bar{\nu}_i}(s)$ at centre-of-mass (cm) energy squared $s = 2\,m_{\nu_i}\,E_{\nu_i}$, the branching ratio $\mathrm{Br}(Z \to \mathrm{hadrons})$, the energy distribution $\mathrm{d}N_{p+n}/\mathrm{d}E_p$ of the produced protons (and neutrons) with energy E_p, and the probability $P_p(r, E_p; E)$ that a proton created at a distance r with energy E_p arrives at Earth above the threshold energy E.

A similar expression as Eq. (11) holds for the differential photon flux from Z-bursts. One simply has to insert the energy distribution of photons from Z-bursts and the photon propagation function. The latter, $P_\gamma(r, E_\gamma; E)$ has a different meaning than that of the proton's. It gives the expected number of detected photons above the threshold energy E if one photon started from a distance of r with energy E_γ.

The building blocks related to Z-production and decay – $\sigma_{\nu_i\bar{\nu}_i}$, the hadronic branching ratio, and the momentum distributions $\mathrm{d}N_i/\mathrm{d}E_i$ – are very well known. The determination of the propagation functions P_i – though CPU intensive – can be done using the precisely known microwave backround spectrum and the fairly well known radio and infrared background spectra. The first two ingredients, the flux of UHECνs, $F_{\nu_i}(E_{\nu_i}, r)$, and the radial distribution of the relic neutrino number density $n_{\nu_i}(r)$ are, however, much less accurately known. In the following all these ingredients are discussed in detail.

3.1. Z production and decay

The s-channel Z-exchange annihilation cross section into any fermion anti-fermion ($f\bar{f}$) pair is given by

$$\sigma^Z_{\nu_i\bar{\nu}_i}(s) = \frac{G_F^2\,s}{4\,\pi}\,\frac{M_Z^4}{(s - M_Z^2)^2 + M_Z^2\,\Gamma_Z^2}\,N_{\mathrm{eff}}(s)\,, \tag{12}$$

where s is the cm energy squared, Γ_Z is the total width of the Z boson, and N_{eff} is the effective number of annihilation channels,

$$N_{\mathrm{eff}}(s) = \sum_f \theta(s - 4\,m_f^2)\,\frac{2}{3}\,n_f\left(1 - 8\,T_{3\,f}\,q_f\,\sin^2\theta_W + 8\,q_f^2\sin^4\theta_W\right)\,. \tag{13}$$

Here the sum is over all fermions with $m_f < \sqrt{s}/2$, with charge q_f (in units of the proton charge), isospin $T_{3\,f}$ ($1/2$ for u, c and neutrinos; $-1/2$ for d, s, b and negatively charged leptons), and $n_f = 1(3)$ for leptons (quarks (q)). With $\sin^2\theta_W = 0.23147(16)$ for the $\sin^2$

of the effective Weinberg angle and $G_F = 1.16639(1) \times 10^{-5}$ GeV^{-2} for the Fermi coupling constant [56], formula (12) gives, at the Z-mass,

$$\sigma(\nu_i\bar{\nu}_i \to Z^* \to \text{all } q\bar{q}) \mid_{s=M_Z^2} \; = 314.9 \text{ nb}\,, \tag{14}$$

$$\sigma(\nu_i\bar{\nu}_i \to Z^* \to \text{all } f\bar{f}) \mid_{s=M_Z^2} \; = 455.6 \text{ nb}\,, \tag{15}$$

with a branching ratio $\sigma(\nu_i\bar{\nu}_i \to Z^* \to \text{all } q\bar{q})/\sigma(\nu_i\bar{\nu}_i \to Z^* \to \text{all } f\bar{f}) \mid_{s=M_Z^2} = 0.6912$, in good agreement with the experimental result [56],

$$\text{Br}(Z \to \text{hadrons}) = (69.89 \pm 0.07)\,\%\,. \tag{16}$$

Note that the cross-section is sharply peaked at the resonance cm energy squared $s = M_Z^2$. Correspondingly, it acts like a δ-function in the integration over the energies E_{ν_i} in Eqn. (11), and we can assume that the UHECν fluxes are constant in the relevant energy region. Thus, introducing the energy-averaged annihilation cross section [1, 5],

$$\langle\sigma_{\text{ann}}\rangle \equiv \int \frac{\mathrm{d}s}{M_Z^2}\,\sigma_{\text{ann}}(s) = 2\,\pi\,\sqrt{2}\,G_F = 40.4 \text{ nb}\,, \tag{17}$$

which is the effective cross section for all neutrinos within $1/2\,\delta E_{\nu_i}^{\text{res}}/E_{\nu_i}^{\text{res}} = \Gamma_Z/M_Z = 2.7\,\%$ of their peak annihilation energy, we can write

$$\int_0^\infty \mathrm{d}E_{\nu_i}\,F_{\nu_i}(E_{\nu_i})\,\sigma_{\nu_i\bar{\nu}_i}(s = 2\,m_{\nu_i}\,E_{\nu_i}) \simeq E_{\nu_i}^{\text{res}}\,F_{\nu_i}(E_{\nu_i}^{\text{res}})\,\langle\sigma_{\text{ann}}\rangle\,. \tag{18}$$

The next ingredient is the energy distribution of the produced protons and photons in Z decay. We combined existing published and some improved unpublished data on the momentum distribution,

$$\mathcal{P}_p\,(x) \equiv \frac{\mathrm{d}N_p}{\mathrm{d}x}\,, \qquad x \equiv \frac{p_p}{p_{\text{beam}}}\,, \tag{19}$$

of protons (p) (plus antiprotons ($\bar{p}$)) in Z decays [57–61], see Fig. 2 (left). The experimental data, ranging down to $x \approx 8 \cdot 10^{-3}$, were combined with the predictions from the modified leading logarithmic approximation (MLLA) [62] at low x. The $p + \bar{p}$ multiplicity is $\langle N_p\rangle = \int_0^1 \mathrm{d}x\,\mathcal{P}_p(x) = 1.04 \pm 0.04$ in the hadronic channel [56].

In the cm system of the Z production the angular distribution of the hadrons is determined by the spin $1/2$ of the primary quarks and thus proportional to $1 + w^2 = 1 + \cos^2\theta$ (here θ is the angle between the incoming neutrinos and the outgoing hadrons [63]). The energy distribution of the produced protons with energy E_p entering the Z-burst spectrum (11),

$$\frac{\mathrm{d}N_p}{\mathrm{d}E_p} = \frac{2}{E_\nu}\,\frac{\mathrm{d}N_p}{\mathrm{d}y} \equiv \frac{2}{E_\nu}\,\mathcal{Q}_p(y)\,, \tag{20}$$

with $y = 2E_p/E_\nu$, is finally obtained after a Lorentz transformation from the cm system to the lab system,

$$\begin{aligned}\mathcal{Q}_p(y) = \sum_{+,-}\frac{3}{8}\int_{-1}^{+1}\mathrm{d}w\,(1+w^2) \\ \times\;\frac{1}{1-w^2}\left|\frac{\pm y - w\sqrt{y^2-(1-w^2)(2m_p/M_Z)^2}}{\sqrt{y^2-(1-w^2)(2m_p/M_Z)^2}}\right| \\ \mathcal{P}_p\left(\frac{-wy \pm \sqrt{y^2-(1-w^2)(2m_p/M_Z)^2}}{1-w^2}\right),\end{aligned} \tag{21}$$

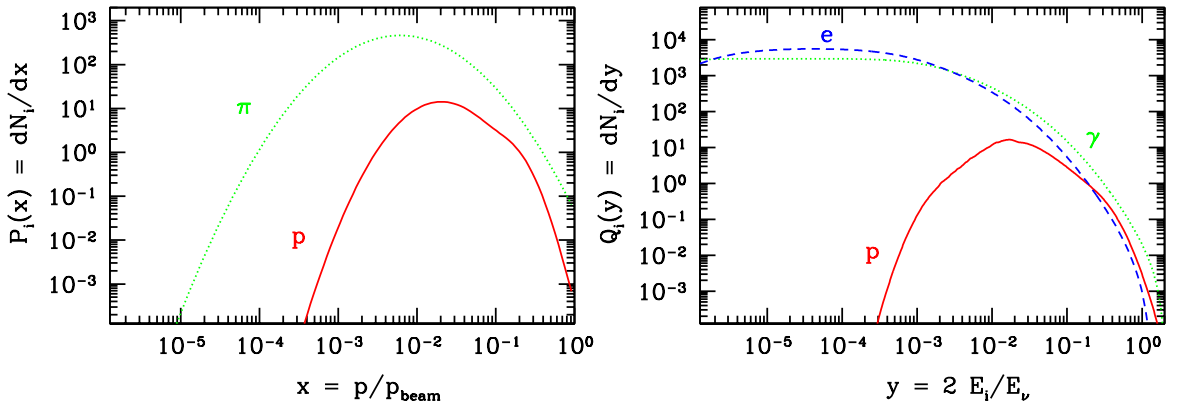

Figure 2. Momentum distributions in hadronic Z decays. *Left:* Combined data from collider experiments on proton (plus antiproton) momentum distribution (solid), normalized to $\langle N_p \rangle = 1.04$, and charged pion momentum distributions (dotted), normalized to $\langle N_{\pi^\pm} \rangle = 16.99$. *Right:* Distribution of protons ("p"; solid), photons ("γ"; dotted) and electrons ("e"; dashed) in the lab system, in which the target relic neutrino is at rest.

where m_p is the proton mass. The first line comes from the angular distribution, the second line is the Jacobian and the third one is the momentum distribution at the inverted momentum. The scaled energy distribution $\mathcal{Q}_p$, as defined in Eq. (20) and given by Eq. (21), is displayed in Fig. 2 (right).

Neutrons produced in Z decays will decay and end up as UHECR protons. They were taken into account according to

$$\mathcal{Q}_{p+n}(y) = \left(1 + \frac{\langle N_n \rangle}{\langle N_p \rangle}\right) \mathcal{Q}_p(y)\,, \tag{22}$$

where the neutron (n) (plus antineutron ($\bar{n}$)) multiplicity, $\langle N_n \rangle = \int_0^2 \mathrm{d}y\, \mathcal{Q}_n(y)$, is $\approx 4\%$ smaller than the proton's.

Photons are produced in hadronic Z decays via fragmentation into neutral pions, $Z \to \pi^0 + X \to 2\,\gamma + X$ (cf. Fig. 1). The corresponding scaled energy distribution in the lab system, defined analogously to Eq. (20), reads

$$\mathcal{Q}_\gamma(y) = \int_{-1}^1 \mathrm{d}w\, \frac{2}{1+w}\, \mathcal{Q}_{\pi^0}\left(\frac{2\,y}{1+w}\right)\,, \tag{23}$$

where the scaled energy distribution $\mathcal{Q}_{\pi^0}(y)$, with $y = 2\,E_{\pi^0}/E_\nu$, is given by Eq. (21), with $m_p \to m_{\pi^0}$ and $\mathcal{P}_p \to \mathcal{P}_{\pi^0}$, the momentum distribution of pions in hadronic Z decay. For the latter distribution, we took the measured one of charged pions $\mathcal{P}_{\pi^\pm}$ from hadronic Z decay [57–61] (cf. Fig. 2 (left)), normalized such that $\langle N_\gamma \rangle = \int_0^2 \mathrm{d}y\, \mathcal{Q}_\gamma(y) = 20.97$ [56].

Electrons (and positrons) from hadronic Z decay are also relevant for the development of electromagnetic cascades. They stem from decays of secondary charged pions, $Z \to \pi^\pm + X \to e^\pm + X$ (cf. Fig. 1), and their scaled energy distribution in terms of $y = 2\,E_e/E_\nu$ reads

$$\mathcal{Q}_{e^\pm}(y) = \int_{-1}^1 dw \int_0^2 dx \frac{1}{xw + \sqrt{x^2 + (2\,m_e/m_\pi)^2}} \tag{24}$$

$$\times\, \mathcal{Q}_{\pi^\pm}\left(\frac{2\,y}{xw + \sqrt{x^2 + (2\,m_e/m_\pi)^2}}\right) \mathcal{P}_e(x)\,,$$

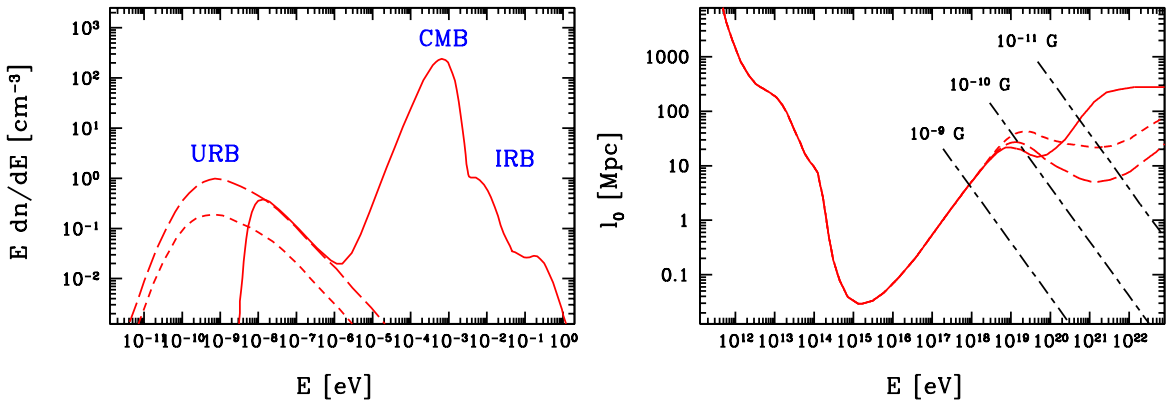

Figure 3. *Left:* The intensity spectrum of the diffuse extragalactic photon background at redshift $z = 0$ (solid). Different estimates of the universal radio background (URB) are also indicated: high URB (long-dashed) and moderate URB (short-dashed). *Right:* Photon energy attenuation length l_0 at $z = 0$ corresponding to the photon background shown on the left (solid). Variations of l_0 arising from different assumptions about the URB are also indicated: high URB (long-dashed) and moderate URB (short-dashed). The energy attenuation length for electrons due to synchrotron radiation for different magnitudes of the extragalactic magnetic fields is also shown (long-dashed-short-dashed).

where $\mathcal{P}_e$ is the momentum distribution of the electrons in the rest system of the charged pion. The energy distribution $\mathcal{Q}_{e^\pm}$ is also displayed in Fig. 2 (right).

3.2. Propagation of nucleons and photons

The cosmic microwave background is known to a high accuracy. It plays the key role in the determination of the probability $P_p(r, E_p; E)$ that a proton created at a distance r with energy E_p arrives at Earth above the threshold energy E, suggested in Ref. [64] and determined for a wide range of parameters in Ref. [65]. The propagation function P_p takes into account the fact that protons of extragalactic (EG) origin and energies above $\approx 4 \cdot 10^{19}$ eV lose a large fraction of their energy due to pion and e^+e^- production through scattering on the CMB and due to their redshift [19, 20]. In our analysis we went, according to

$$\mathrm{d}z = -(1+z)\, H(z)\, \mathrm{d}r/c\,, \tag{25}$$

out to distances $R_{\max}$ (cf. (11)) corresponding to redshift $z_{\max} = 2$. We used the expression

$$H^2(z) = H_0^2 \left[\Omega_M\,(1+z)^3 + \Omega_\Lambda\right] \tag{26}$$

for the relation of the Hubble expansion rate at redshift z to the present one. Uncertainties of the latter, $H_0 = h$ 100 km/s/Mpc, with $h = (0.71 \pm 0.07)\times^{1.15}_{0.95}$ [56], were included. In Eq. (26), Ω_M and Ω_Λ, with $\Omega_M + \Omega_\Lambda = 1$, are the present matter and vacuum energy densities in terms of the critical density. As default values we chose $\Omega_M = 0.3$ and $\Omega_\Lambda = 0.7$, as favored today. Our results turn out to be pretty insensitive to the precise values of the cosmological parameters.

We determined $P_p(r, E_p; E)$ in a range of $r \leq 4000$ Mpc, 10^{18} eV $\leq E_p \leq 10^{26}$ eV, and 10^{18} eV $\leq E \leq 10^{26}$ eV, for several fixed values of the cosmological parameters. The simulation was carried out in small (10 kpc) steps in r. For each step, the statistical energy losses due to pion/e^+e^- production and redshift were taken into account [65]. In this connection, the advantage of our formulation of the Z-burst spectrum in terms of the probability $P_p(r, E_p; E)$ becomes evident. We have to determine the latter only once

and for all. Without the use of $P_p(r, E_p; E)$, we would have to perform a simulation for any variation of the input spectrum, notably for any change in the neutrino mass. Since $P_p(r, E_p; E)$ is of universal usage, we made the corresponding numerical data for the probability distribution $(-)\partial P_p(r, E_p; E)/\partial E$ available for the public via the World-Wide-Web URL *http://www.desy.de/~uhecr*.

The determination of the photon propagation function $P_\gamma(r, E_\gamma; E)$, entering the photon flux prediction, was done as follows. In distinction to the case of the proton propagation function, we used here the continuous energy loss (CEL) approximation which largely simplifies the work and reduces the required computer resources. In the CEL approximation, the energy (and number) of the detected photons is a unique function of the initial energy and distance, and statistical fluctuations are neglected. A full simulation of the photon propagation function will be the subject of a later work.

The processes that were taken into account are pair production on the diffuse extragalactic photon background (cf. Fig. 3 (left)), double pair production and inverse Compton scattering of the produced pairs. We comment also on synchrotron radiation in a possible extragalactic magnetic field (EGMF). For the energy attenuation length of the photons due to these processes, we exploited the values quoted in Ref. [66] (see also Ref. [67]) and the further ones presented in Fig. 3 (right) which incorporate various assumptions about the poorely known universal radio (URB) (from Ref. [68]) and infrared (IRB) backgrounds. We shall analyse later the dependence of the neutrino mass and other fit parameters on these variations. Note, that, in view of the recent URB estimates in Ref. [68], the ones presented in Fig. 3 (left)), which are based on Ref. [69], can be referred to as "minimal" URB.

The computation of the photon propagation function $P_\gamma(r, E_\gamma; E)$ was carried out in the following way. The energy attenuation of photons in the CEL approximation was calculated according to

$$dE = -E\left(\frac{\mathrm{d}r}{l_z(E)} - \frac{\mathrm{d}z}{1+z}\right), \tag{27}$$

where $l_z(E) = (1+z)^{-3}\, l_0(E(1+z))$ is the energy attenuation length at redshift z. The number of photons was assumed to be constant at ultrahigh energies $\gtrsim 10^{18}$ eV, due to the small inelasticities in this energy range. Below, it was increased in a way to maintain energy conservation (except for the redshift contribution):

$$\mathrm{d}N_\gamma = -N_\gamma \frac{\mathrm{d}r}{l_z(E)}\,. \tag{28}$$

The $P_\gamma(r, E_\gamma; E)$ function was then obtained by integration of these equations. In the ultrahigh energy region – which is most relevant for us since we performed our fit to the cosmic ray data there – the approximation described above gives the photon flux quite reliable, while at lower energies it yields an upper bound.

3.3. UHECν fluxes

The differential fluxes F_{ν_i} of UHEνs are unknown. Present experimental upper limits on these fluxes are rather poor. The results of the Fly's Eye [70] and Goldstone lunar ultrahigh energy (GLUE) [71] neutrino experiments are summarized of Fig. 4.

What are the theoretical expectations for diffuse UHECν fluxes? More or less guaranteed are the so-called cosmogenic neutrinos which are produced when ultrahigh energy cosmic protons scatter inelastically off the cosmic microwave background radiation in processes such as $p\gamma \to \Delta \to n\pi^+$, where the produced pions subsequently decay. These fluxes (for recent estimates, see Refs. [3, 67, 72–74]) represent reasonable lower limits, but turn out to be

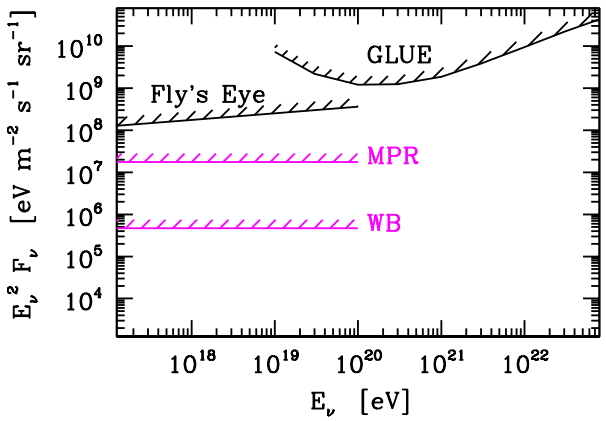

Figure 4. Upper limits on differential neutrino fluxes in the ultrahigh energy regime. Shown are experimental upper limits on $F_{\nu_e} + F_{\bar{\nu}_e}$ from Fly's Eye and on $\sum_{\alpha=e,\mu}(F_{\nu_\alpha} + F_{\bar{\nu}_\alpha})$ from the Goldstone lunar ultrahigh energy neutrino experiment GLUE, as well as theoretical upper limits on $F_{\nu_\mu} + F_{\bar{\nu}_\mu}$ from "visible" ("WB") and "hidden" ("MPR") hadronic astrophysical sources.

insufficient for the Z-burst scenario. Recently, theoretical upper limits on the ultrahigh energy cosmic neutrino flux have been given in Refs. [75–77]. Per construction, the upper limit from "visible" hadronic astrophysical sources, i. e. from those sources which are transparent to ultrahigh energy cosmic protons and neutrons, is of the order of the cosmogenic neutrino flux and shown in Fig. 4 ("WB"; cf. Refs. [75,76]). Also shown in this figure ("MPR") is the much larger upper limit from "hidden" hadronic astrophysical sources, i. e. from those sources from which only photons and neutrinos can escape [77]. A recent detailed simulation showed that these bounds can be exceeded if the spectrum of the source is hard enough [74]. Even larger fluxes at ultrahigh energies may arise if the hadronic astrophysical sources emit photons only in the sub-MeV region – thus evading the "MPR" bound in Fig. 4 – or if the neutrinos are produced via the decay of superheavy relic particles.

In this situation of insufficient knowledge, we took the following approach concerning the flux of ultrahigh energy cosmic neutrinos, $F_{\nu_i}(E_{\nu_i}, r)$. It is assumed to have the form

$$F_{\nu_i}(E_{\nu_i}, r) = F_{\nu_i}(E_{\nu_i}, 0)\,(1+z)^\alpha\,, \tag{29}$$

where z is the redshift and where α characterizes the cosmological source evolution (see also Refs. [3, 23, 37]). The flux at zero redshift, $F_{\nu_i}(E_{\nu_i}, 0) \equiv F_{\nu_i}(E_{\nu_i})$, is left open. For hadronic astrophysical sources it is expected to fall off power-like, $F_{\nu_i}(E_{\nu_i}) \propto E_{\nu_i}^{-\gamma}$, $\gamma \gtrsim 1$, at high energies. Due to this fact and because of the strong resonance peaks in the $\nu_i\bar{\nu}_i$ annihilation cross section (12) at the resonance energies (1), the Z-burst rate will be only sensitive to the flux at the resonant energy of the heaviest neutrino. Of course, the latter may be nearly degenerate with the other neutrino mass eigenstates, $m_{\nu_i} \approx m_\nu$, as it is the case for $m_{\nu_3} \gtrsim 0.1$ eV in a three flavour scenario. Correspondingly, our fit to the UHECR data is sensitive only to

$$F_\nu^{\rm res} = \sum_i \left[F_{\nu_i}(E_{\nu_i}^{\rm res}) + F_{\bar{\nu}_i}(E_{\nu_i}^{\rm res})\right]\,, \tag{30}$$

where the sum extends over the number of mass eigenstates which are quasi-degenerate with the heaviest neutrino. Note, finally, that, independently of the production mechanism, neutrino oscillations result in a uniform F_{ν_i} mixture for the different mass eigenstates i.

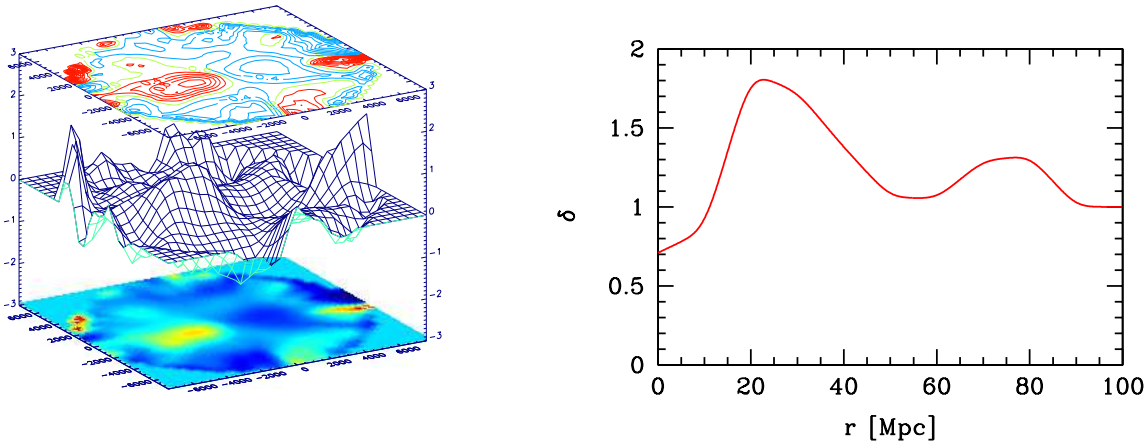

Figure 5. *Left:* Mass density fluctuation field δ along the supergalactic plane as obtained from peculiar velocity measurements. Shown are contours in intervals of $\delta = 0.2$, surface maps on a grid of spacing 500 km s^{-1}, corresponding to $5\,h^{-1}$ Mpc, with the height proportional to δ, and contrast maps. One recognizes some well-known structures in the nearby volume such as the Great Attractor at supergalactic coordinates (SGX ~ -2000 km s^{-1}, SGY ~ -500 km s^{-1}), the Perseus-Pisces complex (SGX $\sim$ 6000 km s^{-1}, SGY ~ -1000 km s^{-1}), and the large void (SGX $\sim$ 2500 km s^{-1}, SGY $\sim$ 0 km s^{-1}) in between. *Right:* Mass density fluctuation field obtained from above data, averaged over all directions, for $h = 0.71$. The overdensities at around 20 and 80 Mpc reflect the Great Attractor and the Perseus-Pisces complex, respectively.

3.4. Neutrino number density

The dependence of the relic neutrino number density n_{ν_i} on the distance r is the last ingredient of the Z-burst spectra.

The main question is whether there is remarkable clustering of the relic neutrinos within the local GZK zone of about 50 Mpc. It is known that the density distribution of relic neutrinos as hot dark matter follows the total mass distribution; however, with less clustering [40, 78, 79]. To take this into account, the shape of the $n_{\nu_i}(r)$ distribution was varied, for distances below 100 Mpc, between the standard cosmological homogeneous case and that of the total mass distribution obtained from peculiar velocity measurements [80] (cf. Fig. 5 (left)). These peculiar measurements suggest relative overdensities of at most a factor $f_\nu = 2 \div 3$, depending on the grid spacing (cf. Fig. 5 (right)). A relative overdensity $f_\nu = 10^2 \div 10^4$ in our neighbourhood, as it was assumed in earlier investigations of the Z-burst hypothesis [4,5,22–24,35], seems unlikely in view of these data. Our quantitative results turned out to be rather insensitive to the variations of the overdensities within the considered range. For scales larger than 100 Mpc the relic neutrino density was taken according to the big bang cosmology prediction, $n_{\nu_i} = 56 \cdot (1+z)^3$ cm^{-3}.

4. Determination of the required neutrino mass and the necessary UHECν flux

Our comparison with the observed spectrum included published UHECR data of AGASA [10], Fly's Eye [11–13], Haverah Park [14, 15], and HiRes [16], as well as unpublished one from the World Wide Web pages of the experiments on 17/03/01. Due to normalization difficulties we did not use the Yakutsk [17] results. The latest HiRes data [81] are not yet included. We shall take into account the fact that above $4 \cdot 10^{19}$ eV less than $50\,\%$ of the cosmic rays can be photons at the $95\,\%$ confidence level (C.L.) [82]

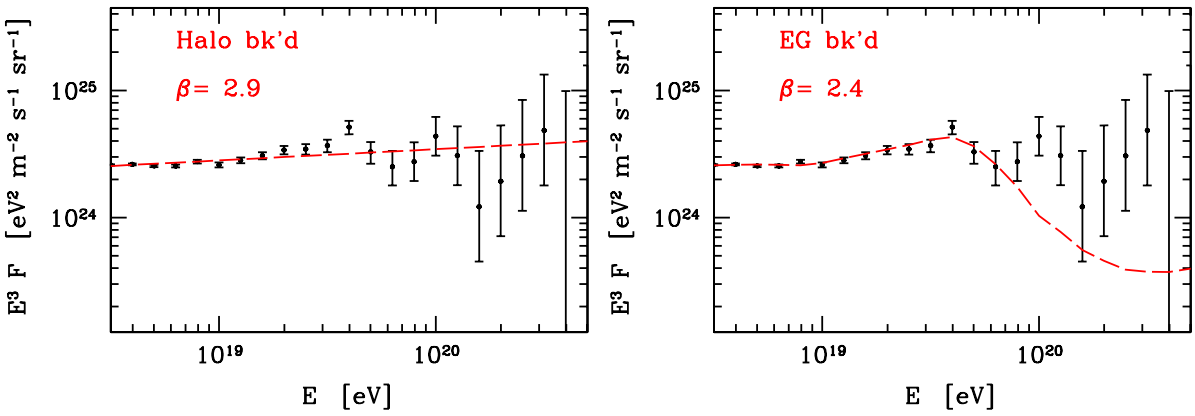

Figure 6. The available UHECR data with their error bars and the best fits (long-dashed) from ordinary cosmic ray protons originating from our local neighbourhood ("halo background"; *left*) and originating from diffuse extragalactic sources ("EG background"; *right*), respectively. For the latter case, the bump at $4 \cdot 10^{19}$ eV represents protons injected at high energies and accumulated just above the GZK cutoff due to their energy losses. The predicted fall-off for energies above $4 \cdot 10^{19}$ eV can be observed.

As usual, each logarithmic unit between $\log(E/\mathrm{eV}) = 18$ and $\log(E/\mathrm{eV}) = 26$ is divided into ten bins. The predicted number of UHECR events in a bin is given by

$$N(i) = \mathcal{E} \int_{E_i}^{E_{i+1}} \mathrm{d}E \left[F_{p|\mathrm{bkd}}(E) + F_{p(+\gamma)|Z}(E) \right], \tag{31}$$

where $\mathcal{E} \approx 8 \cdot 10^{16}$ m$^2 \cdot$ s $\cdot$ sr is the total exposure of the experiments (estimated from the highest energy events and the corresponding fluxes) and where $E_i = 10^{(18+i/10)}$ eV is the lower bound of the i^{th} energy bin. The first term in Eq. (31), $F_{p|\mathrm{bkd}}$, corresponds to the diffuse background of ordinary cosmic rays from unresolved astrophysical sources. Below the GZK cutoff, it should have the usual and experimentally observed power-law form [18]. The second term represents the sum of the proton and photon spectra, $F_{p|Z} + F_{\gamma|Z}$ from Z-bursts.

The separation of the flux into two terms (one from the power-law background and one from the Z-burst) is physically well motivated. The power-law part below the GZK cutoff is confirmed experimentally. For extragalactic sources, it should suffer from the GZK effect. In the Z-burst scenario, cosmic rays are coming from another independent source (Z-bursts), too. What we observe is the sum of the two. As the detailed fits in the next section will show, the flux from Z-bursts is much smaller in the low energy region than the flux of the power-law background. Correspondingly, the low energy part of the spectrum (between $10^{18.5}$ and $10^{19.3}$ eV) has very little influence on the Z-burst fit parameters, notably on the neutrino mass. We investigated three possibilities for the background term $F_{p|\mathrm{bkd}}$.

The first possibility is to assume that the ordinary cosmic rays originate from our galactic halo (or at least from within the GZK zone of about 50 Mpc). This scenario will be referred to as "halo background" in the following. We should note, however, that there are no known astrophysical sources in the arrival directions of the highest energy events. This fact makes this possibility unlikely. In the halo background case the spectrum of ordinary cosmic rays is not distorted by propagation effects, so we can assume the usual power-law behaviour [10, 18] (cf. Fig. 6 (left)),

$$\mathcal{E}\, F_{p|\mathrm{bkd}}(E; A, \beta) = \frac{A}{1\,\mathrm{eV}} \left(\frac{E}{1\,\mathrm{eV}} \right)^{-\beta} \qquad (\mathrm{Halo\ bk'd})\,. \tag{32}$$

The second, most plausible possibility is to assume that the ordinary cosmic rays are protons from uniformly distributed, extragalactic sources – thus we call it "extragalactic

background". In view of the observed, practically uniform distribution of the arrival directions of UHECRs, this assumption seems to be phenomenologically more realistic than the halo background model.

The extragalactic background suffers of course from GZK attenuation. Correspondingly, we take the above power-law (32), $A \cdot E_p^{-\beta}$, as an injection spectrum and determine the final spectrum using the proton propagation function $P_p(r, E_p; E)$,

$$\mathcal{E}\, F_{p|\mathrm{bkd}}(E; A, \beta) = \int_0^\infty \mathrm{d}E_p \int_0^{R_{\max}} \mathrm{d}r\ (1 + z(r))^3 \qquad (33)$$
$$\times\ \frac{A}{1\,\mathrm{eV}} \left(\frac{E_p}{1\,\mathrm{eV}}\right)^{-\beta} (-)\frac{\partial P_p(r, E_p; E)}{\partial E} \quad (\mathrm{EG\ bk'd})\,.$$

The predicted spectrum of the extragactic background protons shows an accumulation at around the GZK scale $4 \cdot 10^{19}$ eV and a sharp drop beyond (see Fig. 6 (right)).

For comparison with recent work on the Z-burst scenario [37], as a third possibility, we have done also fits with no background component, $F_{p|\mathrm{bkd}} = 0$ in Eq. (31), and a larger lower end, $\log(E_{\min}/\mathrm{eV}) = 19.4 \div 20.0$.

The Z-burst part of the predicted flux (31) has several parameters. As it has already been mentioned, this flux is only sensitive to the mass of the heaviest neutrino, this will be denoted in the following by m_ν. The Z-burst spectra can be rewritten as

$$\mathcal{E}\, F_{i|Z}(E; B, m_\nu) = B \int_0^\infty \mathrm{d}E_i \int_0^{R_{\max}} \mathrm{d}r\ (1 + z(r))^{3+\alpha}\ \delta_n(r) \qquad (34)$$
$$\times\ \frac{4\, m_\nu}{M_Z^2}\, \mathcal{Q}_i \left(y = \frac{4\, m_\nu\, E_i}{M_Z^2}\right) (-)\frac{\partial P_i(r, E_i; E)}{\partial E}, \qquad i = p, \gamma\,,$$

where α is the cosmological evolution parameter, $\delta_n(r)$ is the mass density fluctuation field (cf. Fig. 5 (right)), normalized to one, and $\mathcal{Q}_i$ are the boosted momentum distributions from hadronic Z decay, normalized to $\langle N_{p+n}\rangle = 2.04$, for $i = p$, and to $\langle N_\gamma\rangle = 2\,\langle N_{\pi^0}\rangle + \langle N_{\pi^\pm}\rangle = 37$, for $i = \gamma$. After fixing α we have two fit parameters left, the mass m_ν of the heaviest neutrino and the overall normalization B, which may be expressed, using Eqs. (18) and (30), in terms of the original quantities entering the Z-burst spectra, as

$$\frac{B}{\mathcal{E}} = \mathrm{Br}(Z \to \mathrm{hadrons})\, R_{\max}\, \langle n_{\nu_i}\rangle_0\, \langle \sigma_{\mathrm{ann}}\rangle\, E_\nu^{\mathrm{res}}\, F_\nu^{\mathrm{res}}\,. \qquad (35)$$

We can see that the required UHEν flux can easily be obtained from the B parameter. The background term (when it is nonzero) has two parameters, the β exponent and the A normalization factor.

The expectation value for the number of events in a bin is given by Eq. (31). To determine the most probable value for m_{ν_j} we used the maximum likelihood method and minimized [83] the $\chi^2(\beta, A, B, m_\nu)$,

$$\chi^2 = \sum_{\log\left(\frac{E_i}{\mathrm{eV}}\right)=18.5}^{\log\left(\frac{E_i}{\mathrm{eV}}\right)=26.0} 2\,[N(i) - N_{\mathrm{o}}(i) + N_{\mathrm{o}}(i) \ln\left(N_{\mathrm{o}}(i)/N(i)\right)]\,, \qquad (36)$$

where $N_{\mathrm{o}}(i)$ is the total number of observed events in the i^{th} bin. Since the Z-burst scenario results in a quite small flux for lower energies, we took the lower bound just below the "ankle": $E_{\min} = 10^{18.5}$ eV. Our results are insensitive to the definition of the upper end (the flux is extremely small there) for which we chose $\log(E_{\max}/\mathrm{eV}) = 26$. The uncertainties of the measured energies are about 30% which is one bin. Using a Monte Carlo analysis, we took these uncertainties into account and included the corresponding variations in our final error estimates.

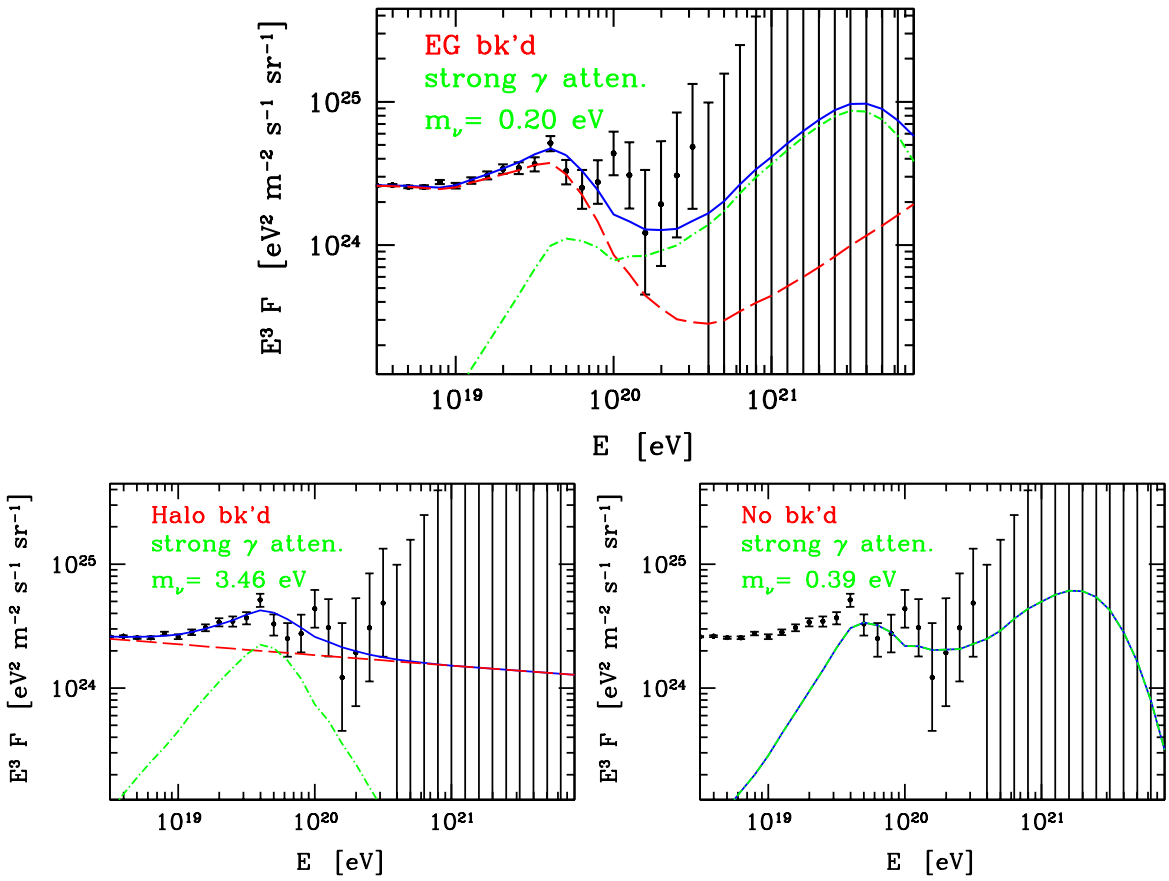

Figure 7. The available UHECR data with their error bars and the best fits from Z-bursts, for a strong UHEγ attenuation such that the Z-burst photons can be neglected ($\alpha = 0, h = 0.71, \Omega_M = 0.3, \Omega_\Lambda = 0.7, z_{\max} = 2$). *Top:* The case of an "extragalactic" UHECR background. The first bump at $4 \cdot 10^{19}$ eV represents protons produced at high energies and accumulated just above the GZK cutoff due to their energy losses. The bump at $2 \cdot 10^{21}$ eV is a remnant of the Z-burst energy. The long-dashed line shows the contribution of the power-law-like spectrum with the GZK effect included. *Bottom left :* Best fit for the case of a halo background (solid line). The bump around $4 \cdot 10^{19}$ eV is mainly due to the Z-burst protons (dash-dotted), whereas the almost horizontal contribution (long-dashed) is the first, power-law-like term of Eq. (31). *Bottom right:* The case of no UHECR background above $\log(E_{\min}/\text{eV}) = 19.7$.

4.1. Fit results

Our fitting procedure involves four parameters: β, A, B and m_ν. The minimum of the $\chi^2(\beta, A, B, m_\nu)$ function is $\chi^2_{\min}$ at $m_{\nu\,\min}$ which is the most probable value for the mass, whereas the $1\,\sigma$ (68%) confidence interval for m_ν is determined by

$$\chi^2(\beta', A', B', m_\nu) \equiv \chi^2_o(m_\nu) = \chi^2_{\min} + 1\,. \tag{37}$$

Here β', A', B' are defined in such a way that the χ^2 function is minimized in β, A and B, at fixed m_ν.

As already mentioned, presently there is no evidence that the observed highest energy cosmic rays are photons. Let us start therefore with the assumption (cf. Ref. [32]) that the ultrahigh energy photons from Z-bursts can be neglected in the fit in comparison to the protons. This is certainly true for a sufficiently large universal radio background, and/or for a

Table 1. Results of fits, for a strong UHEγ attenuation ($h = 0.71, \Omega_M = 0.3, \Omega_\Lambda = 0.7, z_{\max} = 2$). *Top:* Assuming a halo UHECR background according to Eq. (32). *Middle:* Assuming an extragalactic UHECR background according to Eq. (34). *Bottom:* Assuming no UHECR background above $E_{\min}$, for different values of the lower end $E_{\min}$ of the fit ($\alpha = 0$).

EG UHECR background + strong UHEγ attenuation					
α	m_ν [eV]	$\chi^2_{\min}$	A	B	β
-3	$0.20^{+0.20(0.63)}_{-0.11(0.18)}$	25.82	$5.00 \cdot 10^{31}$	150	2.465
0	$0.20^{+0.19(0.61)}_{-0.12(0.18)}$	26.41	$5.98 \cdot 10^{31}$	144	2.466
3	$0.20^{+0.19(0.59)}_{-0.11(0.17)}$	26.89	$7.23 \cdot 10^{31}$	142	2.467
Halo UHECR background + strong UHEγ attenuation					
α	m_ν [eV]	$\chi^2_{\min}$	A	B	β
-3	$4.46^{+2.22(4.80)}_{-1.64(2.88)}$	15.90	$1.46 \cdot 10^{43}$	1049	3.110
0	$3.46^{+1.73(4.03)}_{-1.34(2.32)}$	15.64	$1.62 \cdot 10^{43}$	770	3.111
3	$2.51^{+1.45(3.30)}_{-1.05(1.80)}$	15.53	$1.65 \cdot 10^{43}$	551	3.111
No UHECR background + strong UHEγ attenuation					
$\log(E_{\min}/\text{eV})$	m_ν [eV]	$\chi^2_{\min}$	A	B	β
19.4	$2.28^{+0.64(1.46)}_{-0.58(1.06)}$	21.81	–	1251	–
19.5	$1.31^{+0.63(1.44)}_{-0.53(0.80)}$	16.01	–	846	–
19.6	$0.85^{+0.67(1.62)}_{-0.31(0.55)}$	14.80	–	670	–
19.7	$0.40^{+0.32(0.87)}_{-0.16(0.27)}$	8.03	–	445	–
19.8	$0.42^{+0.41(1.25)}_{-0.18(0.29)}$	7.99	–	460	–
19.9	$0.76^{+1.06(2.50)}_{-0.39(0.58)}$	5.52	–	733	–
20.0	$1.77^{+1.49(3.47)}_{-1.01(1.47)}$	2.68	–	2021	–

sufficiently strong extragalactic magnetic field $\mathcal{O}(10^{-9})$ G. We shall refer to this scenario in the following as "strong" UHEγ attenuation. Our best fits to the observed data for this scenario are given by Table 1. We can see that the required neutrino masses are rather insensitive to the evolution parameter α. The fits can be seen in Fig. 7, for $\alpha = 0$. We found a neutrino mass of $m_\nu = 3.46^{+1.73(4.03)}_{-1.34(2.32)}$ eV for the "halo background" scenario, $m_\nu = 0.20^{+0.19(0.61)}_{-0.12(0.18)}$ eV, if the background is extragalactic, and $m_\nu = 0.40^{+0.32(0.87)}_{-0.16(0.27)}$ eV, if there are are no background protons above $10^{19.7}$ eV. The first numbers are the $1\,\sigma$, the numbers in the brackets are the $2\,\sigma$ errors. This gives an absolute lower bound on the mass of the heaviest neutrino of $m_\nu > 0.02$ eV at the 95% C.L., which is comparable to the one obtained from the atmospheric mass splitting in a three flavour scenario, Eq. (2).

The surprisingly small uncertainties are based on the χ^2 analysis described previously. The inclusion of the already mentioned 30 % uncertainties in the observed energies by a Monte Carlo analysis increases the error bars by about 10 %. Note, that the relative errors in the extragalactic and in the no background cases are of the same order. This clearly shows that the smallness of these errors does not originate from the low energy part of the background component.

The fits are rather good: for 21 non-vanishing bins and 4 fitted parameters they can be as low as $\chi^2_{\min} = 15.64$ and $\chi^2_{\min} = 25.82$ in the halo and the extralactic background case, respectively, whereas in the no background case, for $E_{\min} = 10^{19.7}$ eV, we have 9 bins with

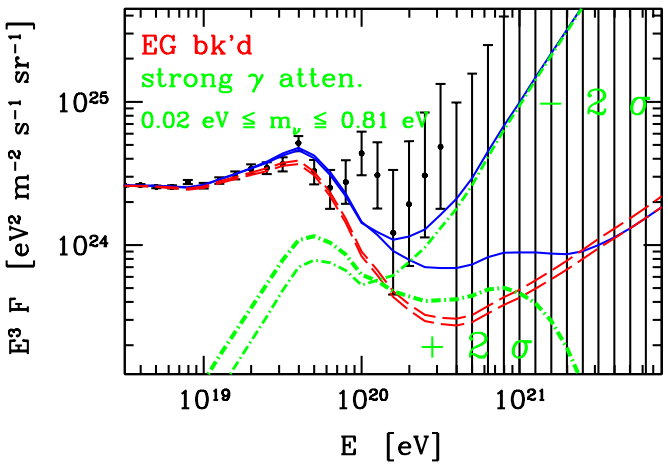

Figure 8. The available UHECR data with their error bars and the $\chi^2_{\rm min} \pm 4$ fits (solid lines) from Z-bursts for an extragalactic UHECR background (long-dashed lines), and a strong UHEγ attenuation such that the Z-burst photons can be neglected and only the Z-burst protons (dash-dotted lines) have to be taken into account in the fit ($\alpha = 0, h = 0.71, \Omega_M = 0.3, \Omega_\Lambda = 0.7, z_{\rm max} = 2$).

Table 2. Results of fits, for a photon attenuation corresponding to "minimal" URB and vanishing EGMF. ($\alpha = 0, h = 0.71, \Omega_M = 0.3, \Omega_\Lambda = 0.7, z_{\rm max} = 2$).

background	m_ν [eV]	$\chi^2_{\rm min}$	A	B	β
EG	$0.77^{+0.48(1.36)}_{-0.30(0.51)}$	24.52	$6.44 \cdot 10^{31}$	120	2.467
Halo	$3.71^{+1.40(3.27)}_{-1.12(1.96)}$	15.36	$1.05 \cdot 10^{44}$	827	3.166

2 fitted parameters and a $\chi^2_{\rm min} = 8.03$, see Table 1. In the latter case, however, a remarkable dependence of the fitted mass on the value of $E_{\rm min}$ is observed. The $\pm 2\ \sigma$ fits are shown in Fig. 8 for the extragalactic case. According to the expectations the spread is small in the region where there are data, whereas it can be quite large in the presently unexplored ultrahigh energy regime.

As the other extreme, let us consider now the case of "minimal" URB on the level of the one in [69] and a vanishing EGMF. Then the photons will give a non-negligible contribution in the ultrahigh energy region. The corresponding fit results for $\alpha = 0$ are given by Table 2 while the best fit for the extragalactic background case is shown by Fig. 9. The values of the neutrino mass found in both the halo background scenario, with $m_\nu = 3.71^{+1.40(3.27)}_{-1.12(1.96)}$ eV, as well as in the extragalactic background scenario, with $m_\nu = 0.77^{+0.48(1.36)}_{-0.30(0.51)}$ eV, are compatible with the corresponding values found in the case of strong UHEγ attenuation.

We also performed the fits for other values of the cosmological parameters and relic neutrino overdensities. We found that for a wide range (e.g. $\alpha = -3 \div 3$, $h = 0.61 \div 0.9$, $z_{\rm max} = 2 \div 5$) the results remain well within the errorbars. The only dependence (still within the errorbars) is caused by the choice of the background and the type of photon propagation (i. e. the strength of the URB and/or EGMF). Fig. 10 contains a summary of the neutrino masses for the extragalactic and halo scenarios and three different photon propagations (the already mentioned strong UHEγ attenuation and the "minimal" URB and a "moderate" URB case in between the two extremes). The overall mass range for the heaviest neutrino in the case of halo background is 2.1 eV $\leq\ m_\nu \leq\ 6.7$ eV at the 68 % C.L., if we take into account the variations

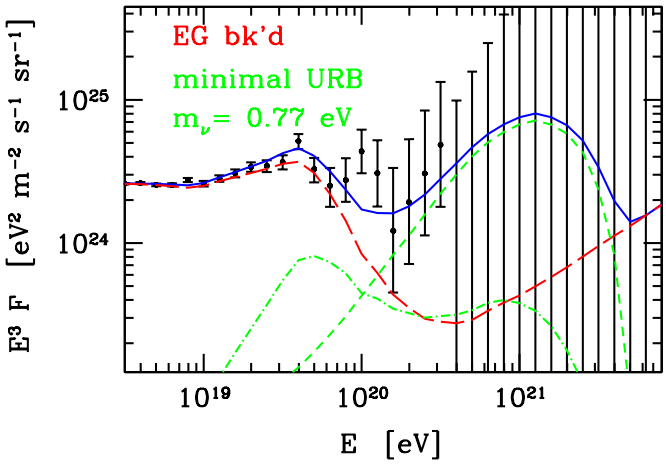

Figure 9. The available UHECR data with their error bars and the best fit from Z-bursts, for an energy attenuation corresponding to "minimal" URB and a vanishing EGMF in the case of extragalactic background. ($\alpha = 0, h = 0.71, \Omega_M = 0.3, \Omega_\Lambda = 0.7, z_{\max} = 2$). The best fit (solid line) is the sum of the contributions of the background protons (long-dashed), the Z-burst protons (dash-dotted) and the Z-burst photons (short-dashed).

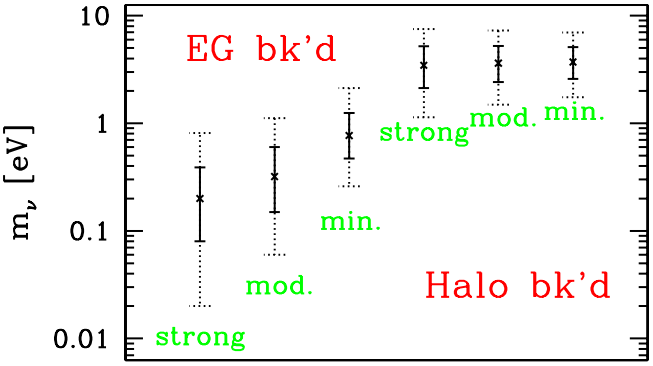

Figure 10. Summary of the masses of the heaviest neutrino required in the Z-burst scenario, with their $1\,\sigma$ (solid) and $2\,\sigma$ (dotted) error bars, for the case of an extragalactic and a halo background of ordinary cosmic rays and for various assumptions about the diffuse extragalactic photon background in the radio band ($\alpha = 0, h = 0.71, \Omega_M = 0.3, \Omega_\Lambda = 0.7, z_{\max} = 2$). From left: strong γ attenuation, moderate and minimal URB.

between the minimal and moderate URB cases and the strong UHEγ attenuation case. For the extragalactic background scenario, the required mass range is 0.08 eV $\leq\ m_\nu \leq\ 1.3$ eV.

Let us consider in more detail the γ ray spectra from Z-bursts, notably in the ~ 100 GeV region. As illustrated in Fig. 11, the EGRET measurements of the diffuse γ background in the energy range between 30 MeV and 100 GeV [84] gives a non-trivial constraints on the evolution parameter α. Whereas the high energy spectrum, and thus the neutrino mass, is independent of α, at low energies only $\alpha \lesssim 0$ seems to be compatible with the EGRET measurements, quite independently of different assumptions about the URB. These numerical findings are in fairly good agreement with other recent simulations [37]. These photon fluxes do not contain any contribution from direct photons emitted by the UHEν sources. As they

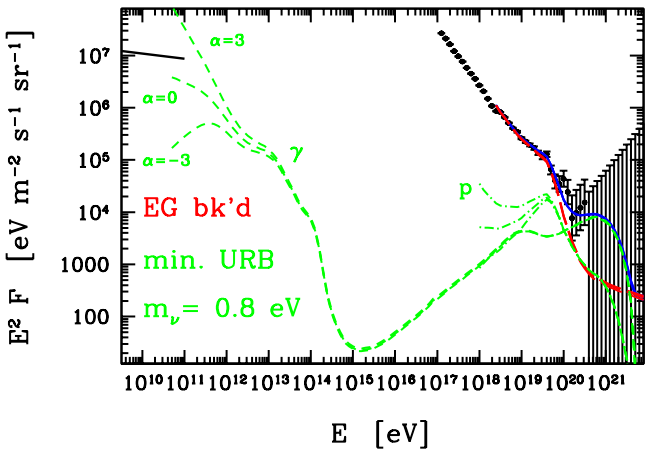

Figure 11. The available UHECR data with their error bars and the best fit from Z-bursts, for various cosmological evolution parameters α and an energy attenuation of photons as in Fig. 3 (bottom) exploiting a "minimal" URB ($h = 0.71, \Omega_M = 0.3, \Omega_\Lambda = 0.7, z_{\rm max} = 2$). Also shown is the diffuse γ background in the energy range between 30 MeV and 100 GeV as measured by EGRET (solid).

are already close to the EGRET limit, one needs special sources that do not give contribution to the EGRET region.

The necessary UHECν flux at the resonant energy $E_\nu^{\rm res}$ is shown by Fig. 12 together with the existing experimental limits and the projected sensitivities of present and future observational projets. They appear to be well below present upper limits and are within the expected sensitivity of AMANDA [85, 86], RICE [87], and Auger [88]. The fluxes are consistent with the ones found in Refs. [37, 38].

The astrophysical sources for the required UHE neutrinos should be distributed with $\alpha \lesssim 0$, accelerate protons up to energies $\gtrsim 10^{23}$ eV, be opaque to primary nucleons and emit secondary photons only in the sub-MeV region. It is an interesting question whether such challenging conditions can be realized in BL Lac objects, a class of active galactic nuclei for which some evidence of zero or negative cosmological evolution has been found (see Ref. [89] and references therein) and which were recently discussed as possible sources of the highest energy cosmic rays [90–92].

It should be stressed that, besides the neutrino mass, the UHECν flux at the resonance energy is one of the most robust predictions of the Z-burst scenario which can be verified or falsified in the near future.

5. Conclusions

We have presented a comparison of the predicted spectra from Z-bursts – resulting from the resonant annihilation of ultrahigh energy cosmic neutrinos with relic neutrinos – with the observed ultrahigh energy cosmic ray spectrum. The mass of the heaviest neutrino should be in the range 2.1 eV $\leq \ m_\nu \ \leq \ 6.7$ eV on the 1 σ level, if the background of ordinary cosmic rays above $10^{18.5}$ eV consists of protons and originates from a region within a distance of about 50 Mpc. In the phenomenologically most plausible case that the ordinary cosmic rays above $10^{18.5}$ are protons of extragalactic origin the required neutrino mass range is 0.08 eV $\leq \ m_\nu \ \leq \ 1.3$ eV at the 68 % C.L.. In the case with no background of ordinary cosmic rays above, say, $10^{19.7}$ eV we found 0.24 eV $\leq \ m_\nu \ \leq \ 2.6$ eV. The above neutrino

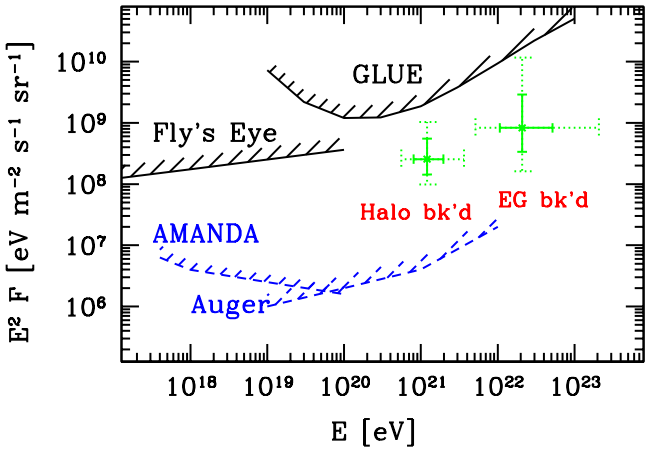

Figure 12. Neutrino fluxes, $F = \frac{1}{3}\sum_{i=1}^{3}(F_{\nu_i} + F_{\bar{\nu}_i})$, required by the Z-burst hypothesis for the case of a halo and an extragalactic background of ordinary cosmic rays, respectively ($\alpha = 0, h = 0.71, \Omega_M = 0.3, \Omega_\Lambda = 0.7, z_{\max} = 2$). Shown are the necessary fluxes obtained from the fit results of Table 1 for the case of a strong UHEγ attenuation. The horizontal errors indicate the $1\,\sigma$ (solid) and $2\,\sigma$ (dotted) uncertainties of the mass determination and the vertical errors include also the uncertainty of the Hubble expansion rate. Also shown are upper limits from Fly's Eye on $F_{\nu_e} + F_{\bar{\nu}_e}$ and GLUE on $\sum_{\alpha=e,\mu}(F_{\nu_\alpha} + F_{\bar{\nu}_\alpha})$, as well as projected sensitivities of AMANDA on $F_{\nu_\mu} + F_{\bar{\nu}_\mu}$ and Auger on $F_{\nu_e} + F_{\bar{\nu}_e}$. The sensitiviy of RICE is comparable to the one of Auger.

mass ranges include variations in presently unknown quantities, like the amount of neutrino clustering, the universal radio background, and the extragalactic magnetic field, within their anticipated uncertainties. There is experimental indication that the highest energy events are mostly not photons. In this special case, when all ultrahigh energy photons are suppressed by a strong enough URB and/or EGMF, the mass range narrows down (with an extragalactic background) to 0.08 eV $\leq\ m_\nu \leq\ 0.40$ eV, with a best fit value of $m_\nu = 0.20$ eV.

It is remarkable, that the mass ranges required for the Z-burst scenario coincide nearly perfectly with the present knowledge about the mass of the heaviest neutrino from oscillations and tritium β decay , $0.04\,\mathrm{eV} \lesssim m_{\nu_3} \lesssim 2.5$ eV, in a three flavour, or $0.4\,\mathrm{eV} \lesssim m_{\nu_4} \lesssim 3.8$ eV, in a four flavour scenario.

It is interesting to observe that the recently reported evidence for neutrinoless double beta decay [46], with $0.11\ \mathrm{eV} \leq \langle m_\nu \rangle \leq 0.56$ eV, if true, is compatible with our "favourite" extragalactic/strong URB scenario.

We also determined the necessary ultrahigh energy neutrino flux at the resonance energy. It was found to be consistent with present upper limits and detectable in the near future by the already operating neutrino telescopes AMANDA and RICE, and by the Pierre Auger Observatory. A search at these facilities is the most promising test of the Z-burst hypothesis.

The required neutrino fluxes are enormous. If such tremendous fluxes of ultrahigh energy neutrinos are indeed found, one has to deal with the challenge to explain their origin. It is fair to say, that at the moment no convincing astrophysical sources are known which meet the requirements for the Z-burst hypothesis, i.e. which have no or a negative cosmological evolution, accelerate protons at least up to 10^{23} eV, are opaque to primary nucleons and emit secondary photons only in the sub-MeV region.

Acknowledgments

We thank the OPAL collaboration for their unpublished results on hadronic Z decays. This work was partially supported by Hungarian Science Foundation grants No. OTKA-T37615/-T34980/T29803/M37071/OMFB1548/OMMU-708.

References

[1] T. Weiler, Phys. Rev. Lett. **49**, 234 (1982).
[2] E. Roulet, Phys. Rev. D **47**, 5247 (1993).
[3] S. Yoshida, H. Y. Dai, C. C. Jui and P. Sommers, Astrophys. J. **479**, 547 (1997).
[4] D. Fargion, B. Mele and A. Salis, Astrophys. J. **517**, 725 (1999).
[5] T. J. Weiler, Astropart. Phys. **11**, 303 (1999).
[6] Y. Fukuda *et al.* [Super-Kamiokande Collaboration], Phys. Rev. Lett. **81**, 1562 (1998).
[7] S. Fukuda *et al.* [SuperKamiokande Collaboration], Phys. Rev. Lett. **86**, 5651 (2001).
[8] Q. R. Ahmad *et al.* [SNO Collaboration], Phys. Rev. Lett. **87**, 071301 (2001).
[9] C. Athanassopoulos *et al.* [LSND Collaboration], Phys. Rev. Lett. **75**, 2650 (1995).
[10] M. Takeda *et al.*, Phys. Rev. Lett. **81**, 1163 (1998).
[11] D. J. Bird *et al.* [HIRES Collaboration], Phys. Rev. Lett. **71**, 3401 (1993).
[12] D. J. Bird *et al.* [HIRES Collaboration], Astrophys. J. **424**, 491 (1994).
[13] D. J. Bird *et al.*, Astrophys. J. **441**, 144 (1995).
[14] M. A. Lawrence, R. J. Reid and A. A. Watson, J. Phys. G **17**, 733 (1991).
[15] M. Ave, J. A. Hinton, R. A. Vazquez, A. A. Watson and E. Zas, Phys. Rev. Lett. **85**, 2244 (2000).
[16] D. Kieda *et al.*, in *Proceedings of the 26th International Cosmic Ray Conference*, Salt Lake, 1999.
[17] N.N. Efimov *et al.*, in *Proc. of the Astrophysical Aspects of the Most Energetic Cosmic Rays* (World Scientific, Singapore, 1991).
[18] M. Nagano and A. A. Watson, Rev. Mod. Phys. **72**, 689 (2000).
[19] K. Greisen, Phys. Rev. Lett. **16**, 748 (1966).
[20] G. T. Zatsepin and V. A. Kuzmin, JETP Lett. **4**, 78 (1966) [Pisma Zh. Eksp. Teor. Fiz. **4**, 114 (1966)].
[21] P. Bhattacharjee and G. Sigl, Phys. Rept. **327**, 109 (2000).
[22] E. Waxman, astro-ph/9804023.
[23] S. Yoshida, G. Sigl and S. J. Lee, Phys. Rev. Lett. **81**, 5505 (1998).
[24] J. J. Blanco-Pillado, R. A. Vazquez and E. Zas, Phys. Rev. D **61**, 123003 (2000).
[25] G. Gelmini and A. Kusenko, Phys. Rev. Lett. **82**, 5202 (1999).
[26] G. Gelmini and A. Kusenko, Phys. Rev. Lett. **84**, 1378 (2000).
[27] T. J. Weiler, hep-ph/9910316.
[28] J. L. Crooks, J. O. Dunn and P. H. Frampton, Astrophys. J. **546**, L1 (2001).
[29] G. B. Gelmini, hep-ph/0005263.
[30] H. Päs and T. J. Weiler, Phys. Rev. D **63**, 113015 (2001).
[31] D. Fargion, M. Grossi, P. G. De Sanctis Lucentini, C. Di Troia and R. V. Konoplich, astro-ph/0102426.
[32] Z. Fodor, S. D. Katz and A. Ringwald, Phys. Rev. Lett. **88**, 171101 (2002)
[33] Z. Fodor, S. D. Katz and A. Ringwald, hep-ph/0105336.
[34] Z. Fodor, S. D. Katz and A. Ringwald, JHEP **0206**, 046 (2002)
[35] B. H. McKellar, M. Garbutt, G. J. Stephenson and T. Goldman, hep-ph/0106123.
[36] A. Ringwald, hep-ph/0111112.
[37] O. E. Kalashev, V. A. Kuzmin, D. V. Semikoz and G. Sigl, Phys. Rev. D **65**, 103003 (2002)
[38] G. Gelmini and G. Varieschi, hep-ph/0201273.
[39] H. Pas and T. J. Weiler, hep-ph/0205191.
[40] S. Singh and C. P. Ma, astro-ph/0208419.
[41] C. Weinheimer *et al.*, Phys. Lett. B **460**, 219 (1999).
[42] V. M. Lobashev *et al.*, Phys. Lett. B **460**, 227 (1999).
[43] J. Bonn *et al.*, Nucl. Phys. Proc. Suppl. **91**, 273 (2001).
[44] C. E. Aalseth *et al.* [IGEX Collaboration], International Germanium Experiment (IGEX) Phys. Rev. C **59**, 2108 (1999).
[45] H. V. Klapdor-Kleingrothaus *et al.*, Eur. Phys. J. A **12**, 147 (2001).
[46] H. V. Klapdor-Kleingrothaus, A. Dietz, H. L. Harney and I. V. Krivosheina, Mod. Phys. Lett. A **16**, 2409 (2002).
[47] S. S. Gershtein and Y. B. Zeldovich, JETP Lett. **4**, 120 (1966) [Pisma Zh. Eksp. Teor. Fiz. **4**, 174 (1966)].
[48] A. D. Dolgov, S. H. Hansen, S. Pastor, S. T. Petcov, G. G. Raffelt and D. V. Semikoz, Nucl. Phys. B **632**, 363 (2002)

[49] A. D. Dolgov, hep-ph/0202122.
[50] S. Hannestad, astro-ph/0208567.
[51] O. Elgaroy *et al.*, Phys. Rev. Lett. **89**, 061301 (2002)
[52] R. A. Croft, W. Hu and R. Dave, Phys. Rev. Lett. **83**, 1092 (1999).
[53] T. J. Loredo and D. Q. Lamb, in *Dallas 1988, Proceedings, Relativistic astrophysics*, pp. 601-630.
[54] P. J. Kernan and L. M. Krauss, Nucl. Phys. B **437**, 243 (1995).
[55] W. Buchmuller, P. Di Bari and M. Plumacher, hep-ph/0209301.
[56] D. E. Groom *et al.* [Particle Data Group Collaboration], Eur. Phys. J. C **15**, 1 (2000).
[57] R. Akers *et al.* [OPAL Collaboration], Z. Phys. C **63**, 181 (1994).
[58] P. Abreu *et al.* [DELPHI Collaboration], Nucl. Phys. B **444**, 3 (1995).
[59] D. Buskulic *et al.* [ALEPH Collaboration], Z. Phys. C **66**, 355 (1995).
[60] K. Abe *et al.* [SLD Collaboration], in *Proc. of the 19th Intl. Symp. on Photon and Lepton Interactions at High Energy LP99*, ed. J.A. Jaros and M.E. Peskin, hep-ex/9908033.
[61] OPAL PN299, unpublished.
[62] Y. I. Azimov, Y. L. Dokshitzer, V. A. Khoze and S. I. Troian, Z. Phys. C **27**, 65 (1985).
[63] M. Schmelling, Phys. Scripta **51**, 683 (1995).
[64] J. N. Bahcall and E. Waxman, Astrophys. J. **542**, 543 (2000).
[65] Z. Fodor and S. D. Katz, Phys. Rev. D **63**, 023002 (2001).
[66] S. Lee, Phys. Rev. D **58**, 043004 (1998).
[67] R. J. Protheroe and P. A. Johnson, Astropart. Phys. **4**, 253 (1996).
[68] R. J. Protheroe and P. L. Biermann, Astropart. Phys. **6**, 45 (1996) [Erratum-ibid. **7**, 181 (1996)].
[69] T. A. Clark, L. W. Brown and J. K. Alexander, Nature **228**, 847 (1970).
[70] R. M. Baltrusaitis *et al.*, Phys. Rev. D **31**, 2192 (1985).
[71] P. W. Gorham, K. M. Liewer, C. J. Naudet, D. P. Saltzberg and D. R. Williams, astro-ph/0102435.
[72] S. Yoshida and M. Teshima, Prog. Theor. Phys. **89**, 833 (1993).
[73] R. Engel and T. Stanev, Phys. Rev. D **64**, 093010 (2001).
[74] O. E. Kalashev, V. A. Kuzmin, D. V. Semikoz and G. Sigl, Phys. Rev. D **66**, 063004 (2002)
[75] E. Waxman and J. N. Bahcall, Phys. Rev. D **59**, 023002 (1999).
[76] J. N. Bahcall and E. Waxman, Phys. Rev. D **64**, 023002 (2001).
[77] K. Mannheim, R. J. Protheroe and J. P. Rachen, Phys. Rev. D **63**, 023003 (2001).
[78] C. P. Ma, astro-ph/9904001.
[79] J. R. Primack and M. A. Gross, astro-ph/0007165.
[80] L. N. da Costa, W. Freudling, G. Wegner, R. Giovanelli, M. P. Haynes and J. J. Salzer, Astrophys. J. **468**, L5 (1996).
[81] T. Abu-Zayyad *et al.* [High Resolution Fly's Eye Collaboration], astro-ph/0208301.
[82] M. Ave, J. A. Hinton, R. A. Vazquez, A. A. Watson and E. Zas, Phys. Rev. D **65**, 063007 (2002)
[83] Z. Fodor and S. D. Katz, Phys. Rev. Lett. **86**, 3224 (2001).
[84] P. Sreekumar *et al.*, Astrophys. J. **494**, 523 (1998).
[85] S. Barwick, talk at RADHEP 2000, UCLA workshop, www.ps.uci.edu/˜amanda
[86] S. Hundertmark *et al.* [AMANDA Collaboration], in *Proc. 27th International Cosmic Ray Conference*, Hamburg, Germany, 2001, pp. 1129-1132.
[87] D. Seckel *et al.* [RICE Collaboration], in *Proc. 27th International Cosmic Ray Conference*, Hamburg, Germany, 2001, pp. 1137-1140.
[88] K. S. Capelle *et al.*, Astropart. Phys. **8**, 321 (1998).
[89] A. Caccianiga *et al.*, astro-ph/0110334.
[90] P. G. Tinyakov and I. I. Tkachev, JETP Lett. **74**, 445 (2001) [Pisma Zh. Eksp. Teor. Fiz. **74**, 499 (2001)]
[91] D. S. Gorbunov, P. G. Tinyakov and S. V. Troitsky, astro-ph/0206385.
[92] A. Y. Neronov and D. V. Semikoz, arXiv:hep-ph/0208248.